Journal of Colloid and Interface Science 515 (2018) 232–239

Contents lists available at ScienceDirect

Journal of Colloid and Interface Science

journal homepage: www.elsevier.com/locate/jcis

Regular Article

High adsorption of methylene blue by salicylic acid–methanol modified steel converter slag and evaluation of its mechanism

Min Cheng, Guangming Zeng *, Danlian Huang *, Cui Lai, Yang Liu, Chen Zhang, Rongzhong Wang, Lei Qin, Wenjing Xue, Biao Song, Shujing Ye, Huan Yi

College of Environmental Science and Engineering, Hunan University, Changsha, Hunan 410082, China
Key Laboratory of Environmental Biology and Pollution Control (Hunan University), Ministry of Education, Changsha, Hunan 410082, China

GRAPHICAL ABSTRACT

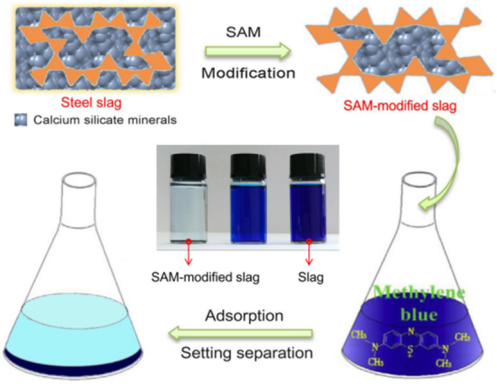

ARTICLE INFO

Article history:
Received 12 November 2017
Revised 23 December 2017
Accepted 3 January 2018
Available online 3 January 2018

Keywords:
Adsorption
Organic pollutants
Methylene blue
Slag
Characterization

ABSTRACT

A novel adsorbent based on steel converter slag (SCS), useful for adsorbing cationic pollutants from water was prepared by a simple method. The characterization showed that salicylic acid–methanol (SAM) modification selectively removed calcium silicate minerals from the surface of SCS and lead to a prominent increase in the specific surface areas. The maximum adsorption capacity of SAM-modified SCS for methylene blue (MB) at initial pH of 7.0 and temperature of 293 K was 41.62 mg/g, which is 35.2-times higher than that of SCS (1.15 mg/g). Adsorption kinetics and isotherms of MB on the SAM-modified SCS can be satisfactorily fitted by pseudo-second order kinetic and Langmuir model, respectively, which suggest that single-layer chemical adsorption was mainly responsible for MB removal. Further studies showed that pH value and ionic strength of wastewater have minimal effects on the adsorption capacity of SAM-modified SCS. A small decrease (<10%) was found in the adsorption capacity of SAM-modified SCS after five cycles. These findings indicate that SAM-modified SCS is a promising adsorbent for the efficient removal of MB from aqueous solution due to its low cost, good thermal stability, excellent adsorption performance and simple separation.

1. Introduction

Water pollution caused by organic compounds is a serious environmental issue, and have attracted much attention

* Corresponding authors at: College of Environmental Science and Engineering, Hunan University, Changsha, Hunan 410082, China.
E-mail addresses: zgming@hnu.edu.cn (G. Zeng), huangdanlian@hnu.edu.cn (D. Huang).

https://doi.org/10.1016/j.jcis.2018.01.008
0021-9797/

worldwide [1–3]. The presence of organic compounds in environmental water can cause serious problems as many of them are potentially toxic and even able to be transformed into teratogenic or carcinogenic agents to life [4–7]. Therefore, the development of effective treatments for the removal of these compounds from the industrial effluents or polluted water is urgently required. The removal of toxic organic compounds from water is in fact a difficult task. Many technologies such as biological treatment [4], chemical oxidation [8], membrane filtration [9] and adsorption [10] have been studied over the years. Among these methods, adsorption has gained particular attention owing to the convenience and simplicity [11–15].

Even though a variety of sorbents are available, there is still a challenge to search for economically feasible, effective and reusable adsorbents with high adsorption capacities. Activated carbon has been proved to be efficient for removing most kinds of organic pollutants form wastewater due to its large specific surface area. However, the operating cost of activated carbon adsorption is high, besides, the separation from the wastewater after process and regeneration of the adsorbent are difficult [16]. The engineered sorbents, such as nanomaterials and supramolecular, have been demonstrated to be effective adsorbents due to their specific morphologies and structures, but many of them suffer from low water dispersibility and high cost [17–20]. Increasing attentions have been paid to the sorbents obtained from waste materials such as agricultural wastes [21–23]. The use of these waste materials for the production of adsorbents not only offers a cheap method for the removal of organic pollutants from waste water, but also resolves the environmental issues [11,24].

Steel slag is a major by-product produced during the production of steel. It was reported that more than 100 million tons of steel slag were discharged in China every year [25,26]. Due to the low utilization rate of steel slag, a large amount of steel slag has been accumulated in China, which leads to the pollution of soils and occupation of farm land [27]. Therefore, improving the utilization rate of steel slag is an imperative way for the steel making industry to realize sustainable development. In addition, steel slag is easy to separate from wastewater after the treatment due to its high density. Thus, the study and application of steel slag for the treatment of wastewater has received much attention. During the past decade, steel slag has been used to remove phosphate [28] and dyes [16] from contaminated water. However, the adsorption capacity of steel slag for dyes is relatively low mainly due to its low specific surface area.

Approximately 1.84 billion metric tonnes of textile-dyeing wastewater was produced in China in 2015 [29]. The presence of synthetic dyestuffs in aquatic ecosystems has gained much attention due to the possibility that they could impact environmental health [30]. In this work, the production and application of a steel slag based adsorbent for the efficient removal of a cationic organic dye methylene blue (MB) from wastewater has been demonstrated. Salicylic acid–methanol (SAM) solution was used to improve the adsorption property of ball-milled steel slag for the first time. A series of mechanical characterizations were applied to reveal the changes in physicochemical properties of the steel slag before and after the modification. The adsorption behaviors of MB to the slag adsorbents, including the adsorption isotherms and kinetics and the factors potentially affecting the adsorption, were investigated. Besides, the renewability evaluation and cost analysis on the production of SAM-modified slag adsorbent were also performed.

2. Experimental section

2.1. Materials and chemicals

The steel converter slag (SCS) used in this study was provided by Valin Iron and Steel Corp (VISTC), Xiangtan, China. The SCS is composed of CaO, SiO_2, FeO, Fe_2O_3, MgO, MnO, Al_2O_3, P_2O_5 and TiO_2 (Table S1). Methylene blue trihydrate ($C_{16}H_{18}ClN_3S.3H_2O$, pKa = 2.6), methanol (CH_3OH, chromatographic grade) and salicylic acid ($C_7H_6O_3$, analytical grade) were obtained from Sinopharm Chemical Reagent (Beijing, China). Ultrapure water (18.3 MΩ cm, Barnstead D11911) was used in all experiments.

2.2. Preparation of sorbent

The raw SCS was grinded with a planetary ball mill (YXQM-4L, MITR, China) and screened while through a 200 mesh sieve to remove the large particles. The obtained SCS powder was fully washed with ultrapure water and dried. 200 g of the dried SCS powder was added in 0.5 L SAM solution (100 g/L) and shaken on a shaking bed with a constant shaking rate of 200 rpm/min at 293 K for 6 h. The mixture was then filtered with the suction filter machine using a 0.45 μm filter membrane. The filtration residue was washed repeatedly with ultrapure water. After drying at 363 K in the oven for 12 h, the SAM solution modified SCS adsorbent (SAM-modified SCS) was obtained.

2.3. Characterization methods

The specific surface area, pore size and pore volume of SCS and SAM-modified SCS were obtained by using the Brunauer-Emmett-Teller (BET) adsorption method (Micromeritics Instrument Corporation, TRI-STAR3020, USA). Their morphology was examined by scanning electron microscope (SEM) scanning (Carl Zeiss, EVO-MA10, Germany) at magnifications of 500 and 3000. Composition analysis of the samples was performed with an energy dispersive X-ray detector (EDX, Oxford Instruments, UK). The crystal phase of the adsorbents was determined by using Cu Kα radiation (λ = 0.15406 nm) in the region of 2θ from 5° to 80° with a D/max-2500 X-ray diffractometer (XRD; Rigaku, Japan). The zeta potentials of SAM-modified SCS in water solutions at different pH were determined with a Zetasizer Nano-ZS90 (Malvern, UK) zeta potential meter. The thermal stability of the prepared slag adsorbents was tested by the thermogravimetric analysis (TGA) with a Mettler TGA/DSC1 analyzer (Columbus, USA). The Fourier transform infrared (FT-IR) spectra of the slag adsorbents were obtained from a Nicolet 5700 Spectrometer (Nicolet, USA).

2.4. Adsorption of MB

The adsorption characteristics of the prepared adsorbents were evaluated by adsorption experiments using MB solution. The initial MB concentrations used in this study were 200 mg/L for kinetics experiments and 10–400 mg/L for isotherms experiments. All batch experiments were performed using 150 mL glass conical flasks containing 100 mg of adsorbent and 50 mL of MB solution, which were stirred in a water bath shaker at 180 rpm and 293 K, unless otherwise noted. The desired pH value of MB solution was adjusted 1 mol/L NaOH or HCl solution. The regeneration of SAM-modified SCS was conducted by heating MB-loaded sorbent at 573 K for 3 h and putting the sorbent to SAM solution (100 g/L) and shaken on a shaking bed with a constant shaking rate of 200 rpm/min at 293 K for 1 h. After which, the suspension liquid was kept standing for 30 min and precipitant was collected and dried in an oven at 353 K for reuse.

After adsorption, 1 mL of the suspension was sampled out and filtrated by 0.45 μm filters. MB concentration was determined by measuring the absorbance of 664 nm with a UV-2700 spectrophotometer (SHIMADZU, Japan). The adsorbed amount of MB on SCS and SAM-modified SCS was calculated as follow:

$$Q_e = (C_0 - C_e)\,V/m \quad (1)$$

where Q_e is the adsorption quantity of MB on SCS or SAM-modified SCS (mg/g); C_0 and C_e are the initial concentration and the equilibrium concentration of MB (mg/L), respectively; V is the volume of MB solution (L), and m is the weight of SCS or SAM-modified SCS (g).

2.5. Mathematical models

The pseudo-first Eq. (2) [31] and pseudo-second order Eq. (3) [32] were adopted to study the adsorption kinetics.

$$\log(Q_e - Q_t) = \log Q_e - k_f \cdot t/2.303 \quad (2)$$

$$t/Q_t = 1/k_s Q_e^2 + t/Q_e \quad (3)$$

where Q_t and Q_e are the adsorbed amount (mg/g) of MB on adsorbents at the initial and equilibrium, respectively. k_f and k_s are the pseudo-first rate constant (1/h) and the pseudo-second rate constant (g/mg h), respectively.

The Langmuir isotherms (4) [33] and Freundlich isotherms (5) [34] were used to study the adsorption isotherms.

$$Q_e = Q_{max} \times K_L \times C_e/(1 + K_L C_e) \quad (4)$$

$$Q_e = K_F C_e^n \quad (5)$$

where Q_e and C_e are adsorbed value (mg/g) of MB and concentration (mg/L) of MB at equilibrium, respectively. K_L is the Langmuir constant (L/mg) and K_F is Freundlich constant ($mg^{1-n}\,L^n\,g^{-1}$). Q_{max} is the maximum adsorption capacity (mg/g) of the adsorbent, and n is the degree of dependence of sorption capacity with equilibrium concentration.

3. Results and discussion

3.1. Physicochemical characterization of the adsorbents

The prepared adsorbents were characterized via different methods. Firstly, the surface morphology of the prepared adsorbents was investigated by BET analysis (Table S2). The result showed that specific surface areas of SCS increased from 5.788 to 66.655 m^2/g. The huge increase in specific surface areas revealed that SAM modification significantly changed the morphology of SCS. On the other hand, the hysteresis of SAM-modified SCS was observed (Fig. S1), indicating that SAM-modified SCS presented the larger number of mesoporous compared to SCS. BET analysis suggested that the modified SCS may have higher adsorption capacity for MB as compared to SCS.

SEM was applied to further study the morphologies changes of SCS. As shown in Fig. 1a and b, the surface of untreated SCS was relatively flat and smooth. After SAM treatment, there was a noticeable change in the surface morphology of SCS, the surface area of SCS was remarkably increased by forming more holes and cracks (Fig. 1c and d). EDX analysis showed that of the unmodified SCS mainly consists of O, Ca, Fe, Si and Mg (Fig. S2a). After SAM modification, a distinct variation in the signal of these elements was

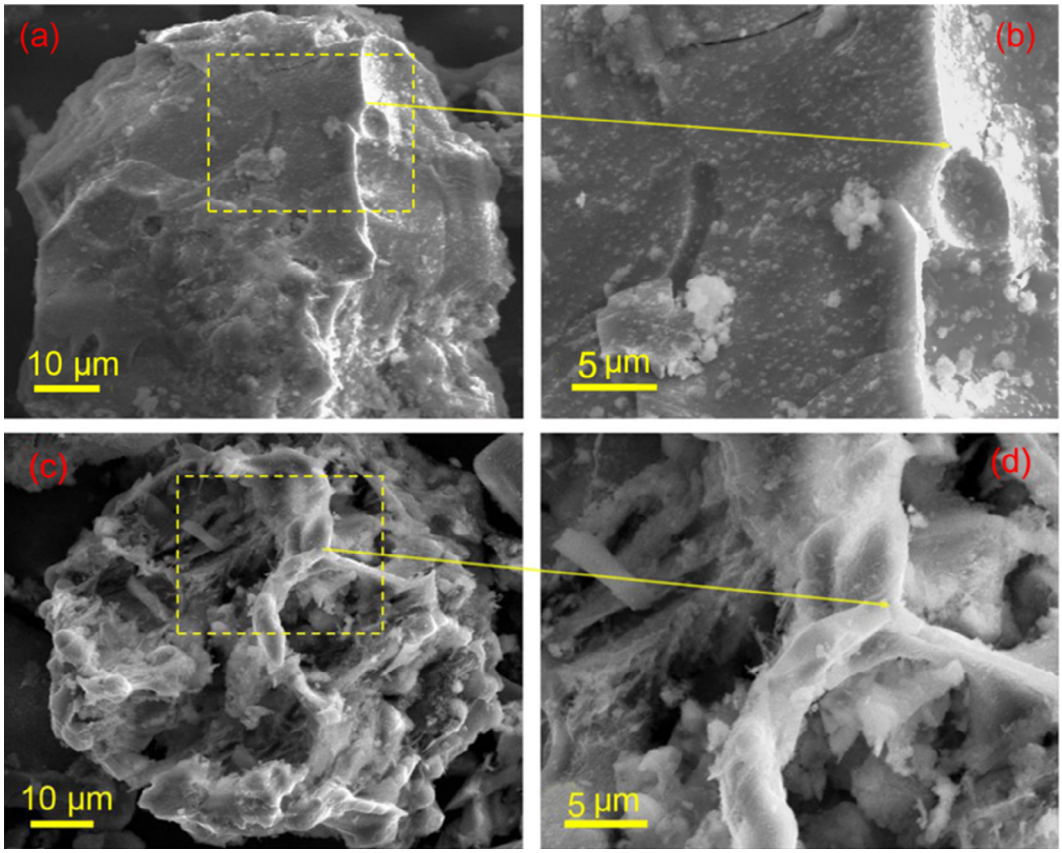

Fig. 1. SEM images of SCS (a, b) and SAM-modified SCS (c, d).

observed (Fig. S1b). The contents of Ca and Si were obviously decreased, while Fe content was tremendously increased after SAM modification. In particular, the mass ratio of Ca to Fe was decreased from 2.70 to 1.08 after SAM modification (Table S2). EDX analysis indicated that the formation of holes on the surface of SCS was likely due to that calcium silicate minerals were selectively removed by SAM treatment.

In order to verify above speculation, the crystal phase of SCS and SAM-modified SCS was analyzed XRD. As can be seen in Fig. 2, the intensities of dicalcium silicate peaks (2θ; 32.02°, 32.92° and 41.09°, JCPDS 49-1673) and tricalcium silicate peaks (2θ; 32.50°, JCPDS 49-0442) prominently decreased after SAM modification. On the contrary, the intensities of iron oxides peaks (2θ; 36.31°, 42.05°, 61.36° and 73.03°, JCPDS 74-1880) of the modified SCS were enhanced as compared to those of unmodified SCS. XRD analysis indicated that the SAM modification removed a portion of calcium silicate minerals from SCS.

TGA of SCS and SAM-modified SCS was conducted to evaluate the thermal stability of the prepared adsorbents. Two mass loss stages were observed from the TGA curve. As shown in Fig. S3, the first step (approximately 2.5% and 2.6% weight loss for SCS and SAM-modified SCS, respectively) was observed from 20 to 200 °C, with the associated derivative weight peak centered at approximately 100 °C, should be due to the dehydration of the samples. Approximately 3.6% and 3.8% weight loss for SCS and SAM-modified SCS, respectively, at 450–710 °C correspond to hydroxide dehydration [35]. Taken together, the SCS based adsorbents exhibited good thermal stability.

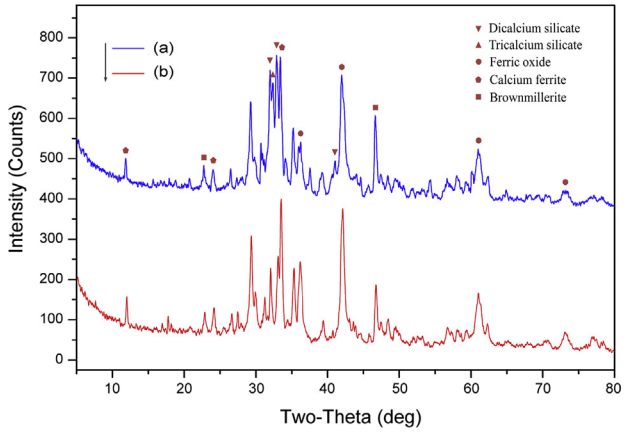

Fig. 2. XRD patterns of SCS (a) and SAM-modified SCS (b). 2θ from 5° to 80°.

3.2. Adsorption kinetics

Fig. 3 shows the adsorption kinetics of MB onto SCS and modified SCS. In the both system, adsorption quantity of MB increased quickly in 30 min and achieved adsorption equilibrium within 3 h. It is noted that the adsorptions of MB on SAM-modified SCS are much higher than SCS. It was concluded that the saturated MB adsorption capacity of the modified SCS was 35.3 times over that of the original SCS. The significant increase in the adsorption capacity for MB is mainly attributed to the changes of surface structure and chemical composition of SCS. As shown in Table S2 and Fig. 1, the surface area and total pore volume of SCS increased significantly after SAM modification. We used the pseudo-first-order and pseudo-second-order kinetic equations to fit the data of sorption kinetics (Fig. 3a and b). It was found that the sorption kinetics of MB on SCS and SAM-modified SCS can be better fitted by the pseudo-second order kinetic model ($R^2 = 0.9942$ and 0.9997, respectively (Table 1)), suggesting chemisorption is the rate-limiting step for adsorption [36].

3.3. Adsorption isotherms

Fig. 4 shows the relationships between equilibrium MB concentration (C_e) and the equilibrium adsorption capacity (Q_e) at different temperatures (293 K, 303 K and 313 K). It was found that the adsorption of MB can be largely affected by temperature. The results showed Q_e increased along with the increases of operating temperature, which indicated that the adsorption of MB onto SAM-modified SCS is an endothermic process. The adsorption isotherms for MB adsorbed by SAM-modified SCS were studied with Langmuir and Freundlich models. As can be seen in Fig. 4b and Table 2, that Langmuir model gives a better fit than Freundlich model. The high correlation coefficients ($R^2 \geq 0.9943$) of Langmuir model for all temperatures tested suggest that single-layer adsorption occurred in MB removal with SAM-modified SCS [37,38].

3.4. FT-IR analysis

FT-IR spectra of the samples were used to further study the adsorption of MB by SAM-modified SCS. The FT-IR spectra of SCS and SAM-modified SCS are similar (Fig. 5a and b). The broad bands in the range 1400–1500 cm^{-1} and 800–1000 cm^{-1} are associated

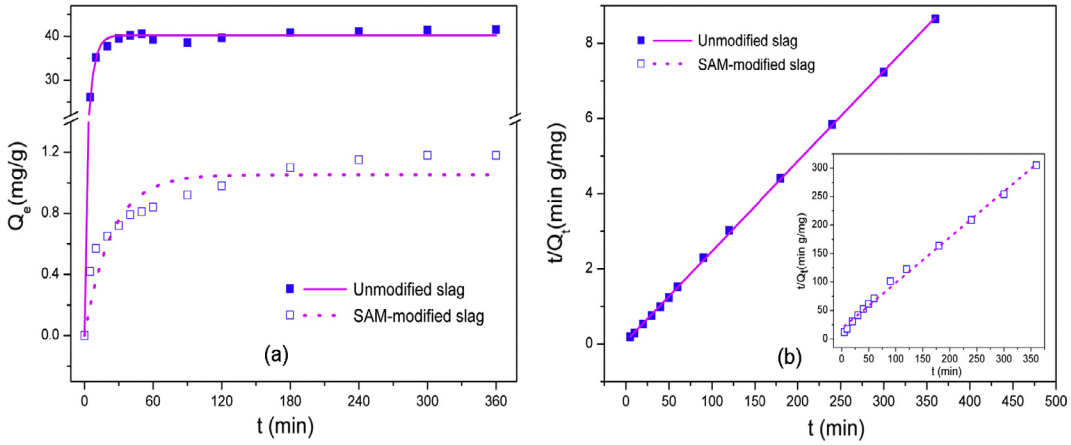

Fig. 3. The adsorption kinetics of MB on SCS and SAM-modified SCS. The lines are the curve fitting using pseudo-first-order kinetic model (a) and pseudo-second-order kinetic model (b). C_0 = 200 mg/L, initial pH = 7.0, m/v = 2 g/L, T = 293 K.

Table 1
The calculated parameters of the pseudo-first order and pseudo-second order kinetic models.

Samples	Pseudo-first order			Pseudo-second order		
	Q_e	k_f (1/h)	R^2	Q_e	k_s (g/mg h)	R^2
SCS	1.06	0.042	0.8402	1.25	3.50×10^{-2}	0.9942
Modified SCS	40.2	0.206	0.9931	43.5	7.56×10^{-3}	0.9997

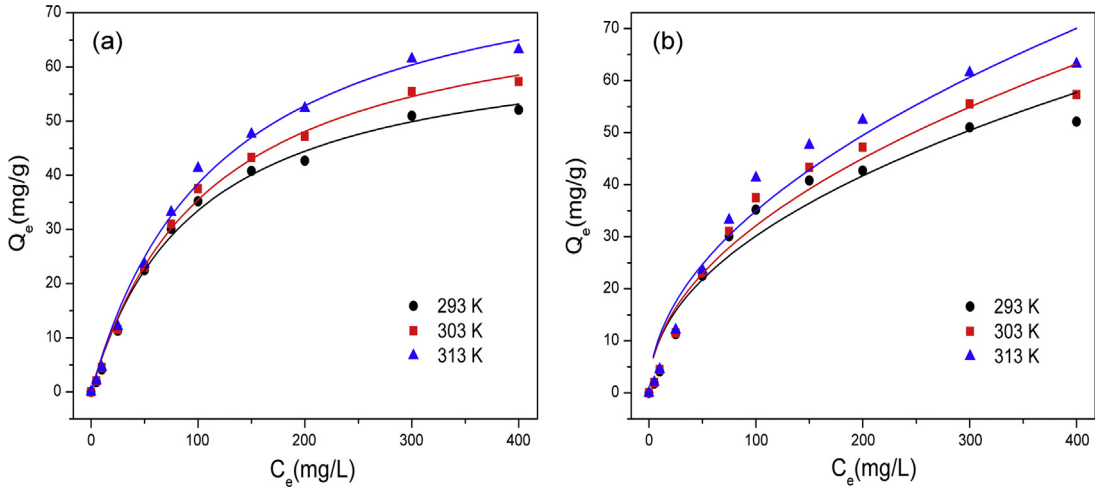

Fig. 4. The equilibrium isotherms for MB adsorbed by SAM-modified SCS at different temperature (293 K, 303 K and 313 K): (a) the Langmuir model; (b) the Freundlich model. Initial pH = 7.0, m/v = 2 g/L.

Table 2
Isotherm parameters for the adsorption of MB onto SAM-modified SCS.

Isotherms	Parameters	Temperature (K)		
		293	303	313
Langmuir	Q_{max} (mg/g)	66.1	74.7	84.5
	K_L (L/mg)	1.03×10^{-2}	9.03×10^{-2}	8.35×10^{-3}
	R^2	0.9943	0.996	0.995
Freundlich	n	0.469	0.488	0.501
	K_F ($mg^{1-n} L^n g^{-1}$)	3.48	3.39	3.34
	R^2	0.9340	0.945	0.944

to the typical stretching vibrations of Ca—O and Si—O, respectively [39,40]. As for pure MB (Fig. 5d), the stretching band of C=N on the benzene ring occurs at 1586 cm^{-1}, and the C—N bending vibration of the N atom connected with the benzene ring is observed at 1323 and 1135 cm^{-1} [10]. After adsorption, C—S stretching vibration at 1028 cm^{-1} from MB was detected in MB-loaded SAM-modified SCS (Fig. 5c). Compared with SAM-modified SCS or MB alone, some obvious variations in characteristic absorption peaks were detected in MB-loaded SAM-modified SCS. First, the characteristic peak at 1586 cm^{-1}, originating from C=N stretching band, shifted to 1613 cm^{-1}. Besides, the Si—O vibrations in the region of 890–980 cm^{-1} from SAM-modified SCS disappeared after the adsorption of MB. These variations in the spectrum varied that chemical adsorption was mainly responsible for MB removal.

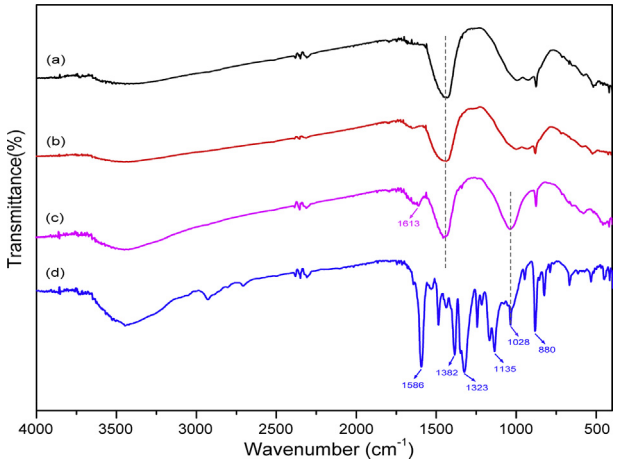

Fig. 5. FT-IR spectra of SCS (a), SAM-modified SCS (b), MB loaded SAM-modified SCS (c) and MB.

3.5. Effect of pH and ionic strength on adsorption efficiency of MB

The solution pH is one of the most important parameters affecting the adsorption behavior [41,42]. The adsorption directly depends on the surface charge of the adsorbents, and the charge is determined by the pH of solution [43]. Fig. 6a shows the changes in the zeta potential values of SAM-modified SCS with pH. At all the measured pH values except 2, SAM-modified SCS had negative zeta potential values, and the zeta potential decreases with pH increasing from 2 to 12. Similar results have been reported by Duan and

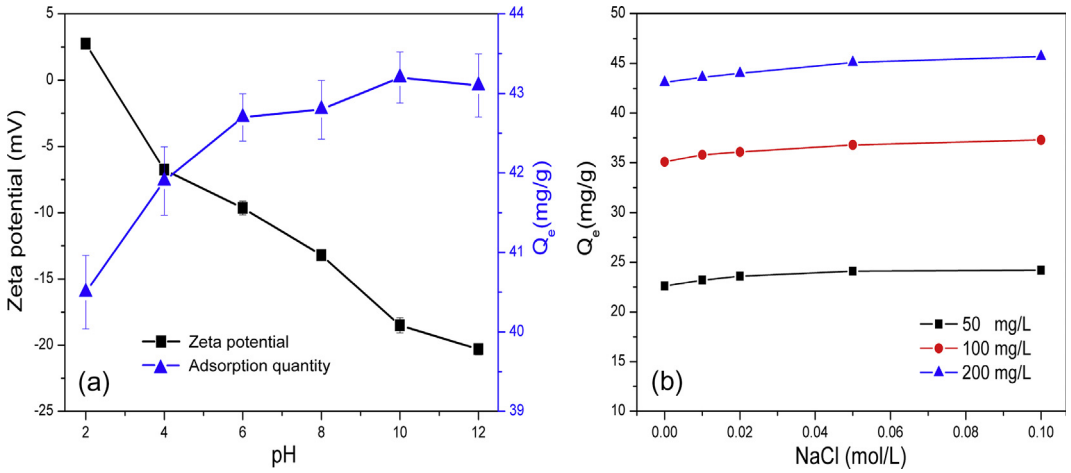

Fig. 6. Effect of initial pH (a) and ionic strength (b) on adsorption of MB by SAM-modified SCS. C_0 = 200 mg/L, initial pH = 7.0, m/v = 2 g/L, T = 293 K.

Su [44], who suggested that only at strong acidic medium, the surface of the slag adsorbent would be protonated with H^+. As the solution pH increased, the negative charges increased, which could enhance the adsorption of positively charged MB cations by electrostatic attraction [10]. In the present study, however, the adsorption of MB on SAM-modified SCS is independent of pH at pH ranged from 2.0 to 12.0. Q_e only varied from 40.5 mg/g to 43.1 mg/g in the tested pH range, indicting the initial pH value has a minimal effect on the adsorption. For further investigation of the effect of SAM-modified SCS on solution pH, the variations of solution pH during the experiment were monitored. As shown in Fig. S4, the pH values in all 5 groups reached equilibrium in 2 h, and maintained in the range of 9.0–9.5. Results indicated that SAM-modified SCS could act as a pH buffer [44] and thus can be applied to treat MB effluent over a wide pH range.

As high concentration of salts is often included in MB effluent, and salt ionic strength could affect the adsorption removal of MB [10]. To reveal the effect of salts on the adsorption performance of SAM-modified SCS, the experiments were carried out with NaCl concentration ranging from 0 to 0.1 mol/L. As displayed in Fig. 6b, a slightly increase in the adsorption MB on SAM-modified SCS was observed with increasing NaCl concentration in this experiment. This is because the salt can positively affect the dissociation of MB molecules to MB^+ and thus promote the electrostatic interaction between the negatively charged adsorbent and MB cations [10,45]. The experimental results suggested that SAM-modified SCS can be used for the treatment of industrial MB wastewater with a high concentration of salts.

3.6. Implication for water purification

Our results suggest the modified SCS is a highly promising adsorbent for removal of MB and other organic contaminant from wastewater, due to its ideal physical characteristics (e.g.,

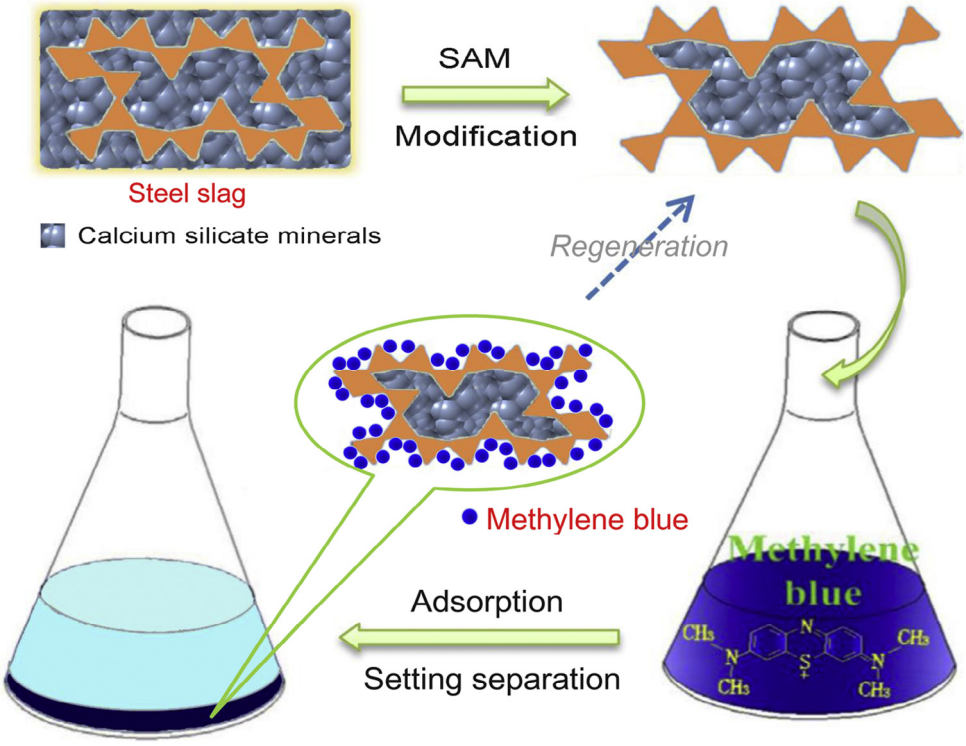

Fig. 7. Schematic depiction of the produce of SAM-modified SCS and application for removal of MB.

high thermal stability, large surface area) and excellent adsorption capacity. The analysis showed SAM-modification enormously increased the surface area and pore volume of SCS, thus providing more adsorption sites for MB removal (Fig. 7). As shown in Fig. 3, the maximal MB adsorption capacity of SAM-modified SCS is 41.62 mg/g at 293 K, which is about 35-times higher than that of the original SCS. Furthermore, this value is also comparable with some well-studied adsorbents such as carbon nanotube (46.2 mg/g) [46] and powdered activated carbon (91.00 mg/g) [47]. Also, the adsorption capacity of modified SCS is barely affected by both the ionic strength and pH of the wastewater. By comparison, most of the other adsorbents cannot deal with low pH wastewater directly. For example, the adsorption capacity of modified graphene oxide declined 42.4% when changing MB solution pH value from 11 to 2 [10]. The versatility of this method is also enhanced by the fact that the adsorbent and the liquid can be easily separated by a settling process after the treatment, which enables the reuse of the adsorbent (Fig. 7).

3.7. The cost analysis and renewability evaluation

The wholesale price of grinded SCS is only about US$ 150 t^{-1} and other chemicals used in this study can be cheaply provided by the industrial supplies. Comparison with the other adsorbents such as carbon nanotubes (US$ 441.85×10^6 t^{-1}) [48], modified graphene oxide (about US$ 60×10^4 t^{-1}) [10] and coconut shell-based activated carbon (US$ 1.32×10^3 t^{-1}) [49], the cost of SAM-modified SCS is much lower. The renewability of adsorbents is an important in practical applications. In this study, the equilibrium adsorption amount of SAM-modified SCS for MB at C_0 = 200 mg/L reduces from 42.15 mg/g to 38.92 mg/g after five cycles (Fig. S5). The slight decline in the adsorption capacity (<10%) suggests that the SAM-modified SCS showed a good reusability. In addition, SEM and XRD were used to study the chemical stability of the absorbent. SEM images of the regenerated absorbent (Fig. S6) are very similar to those of the fresh SAM-modified SCS (Fig. 1c and d), indicating no obvious change occurred in the morphology of the absorbent during adsorption and regeneration processes. It was also noted that there was no significant changes in XRD patterns of SAM-modified SCS before and after the 5-cycle runs (Fig. S7), indicating that the crystal structure of the SAM-modified SCS was stable during the processes. From the above points, we can conclude that the SAM-modified SCS is a promising adsorbent for the removal of MB from wastewater.

4. Conclusions

A cheap adsorbent with high adsorption capacity is produced from steel slag by one-step modification and applied for the removal of MB from wastewater. The characterization of SCS and SAM-modified SCS indicated that calcium silicate minerals in SCS surface were selectively removed by SAM modification. The as-prepared SAM-modified SCS has a high specific surface area and negative charged surface in a wide pH range (3.0–12.0). The maximum adsorption capacity of SAM-modified SCS for MB at initial pH 7.0 and 293 K was 41.62 mg/g, which is much higher than that of SCS (1.15 mg/g). The adsorption process of MB can be well fitted by pseudo second-order kinetic and Langmuir model, suggesting single-layer chemical adsorption was mainly responsible for MB removal. Our results show that SAM-modified SCS can be a promising adsorbent to remove MB from wastewater.

Acknowledgements

This study was financially supported by the Program for the National Natural Science Foundation of China (51579098, 51521006, 51378190, 51408206), the National Program for Support of Top-Notch Young Professionals of China (2014), the Program for Changjiang Scholars and Innovative Research Team in University (IRT-13R17), the Program for New Century Excellent Talents in University (NCET-13-0186), the Hunan Provincial Innovation Foundation for Postgraduate (CX2016B132, CX2017B098), Hunan Provincial Science and Technology Plan Project (No. 2016RS3026) and Shanghai Tongji Gao Tingyao Environmental Science and Technology Development Foundation.

Appendix A. Supplementary material

Supplementary data associated with this article can be found, in the online version, at https://doi.org/10.1016/j.jcis.2018.01.008.

References

[1] J.L. Gong, B. Wang, G.M. Zeng, C.-P. Yang, C.G. Niu, Q.Y. Niu, W.J. Zhou, Y. Liang, Removal of cationic dyes from aqueous solution using magnetic multi-wall carbon nanotube nanocomposite as adsorbent, J. Hazard. Mater. 164 (2) (2009) 1517–1522.
[2] G. Zeng, M. Chen, Z. Zeng, Shale gas: surface water also at risk, Nature 499 (7457) (2013). 154-154.
[3] M. Cheng, G. Zeng, D. Huang, C. Lai, Y. Liu, P. Xu, C. Zhang, J. Wan, L. Hu, W. Xiong, C. Zhou, Salicylic acid–methanol modified steel converter slag as heterogeneous Fenton-like catalyst for enhanced degradation of alachlor, Chem. Eng. J. 327 (2017) 686–693.
[4] G. Zeng, M. Cheng, D. Huang, C. Lai, P. Xu, Z. Wei, N. Li, C. Zhang, X. He, Y. He, Study of the degradation of methylene blue by semi-solid-state fermentation of agricultural residues with Phanerochaete chrysosporium and reutilization of fermented residues, Waste Manage. 38 (2015) 424–430.
[5] Y. Zhang, G.M. Zeng, L. Tang, D.L. Huang, X.Y. Jiang, Y.N. Chen, A hydroquinone biosensor using modified core–shell magnetic nanoparticles supported on carbon paste electrode, Biosensors Bioelectron. 22 (9) (2007) 2121–2126.
[6] M. Cheng, G. Zeng, D. Huang, C. Yang, C. Lai, C. Zhang, Y. Liu, Tween 80 surfactant-enhanced bioremediation: toward a solution to the soil contamination by hydrophobic organic compounds, Crit. Rev. Biotechnol. 1–14 (2017).
[7] D.A. Giannakoudakis, T.J. Bandosz, Zinc (hydr)oxide/graphite oxide/AuNPs composites: role of surface features in H2S reactive adsorption, JCIS 436 (Suppl. C) (2014) 296–305.
[8] M. Cheng, G. Zeng, D. Huang, C. Lai, P. Xu, C. Zhang, Y. Liu, Hydroxyl radicals based advanced oxidation processes (AOPs) for remediation of soils contaminated with organic compounds: a review, Chem. Eng. J. 284 (2016) 582–598.
[9] C. Yu, W. Zhou, H. Liu, Y. Liu, D.D. Dionysiou, Design and fabrication of microsphere photocatalysts for environmental purification and energy conversion, Chem. Eng. J. 287 (2016) 117–129.
[10] Z. Wu, H. Zhong, X. Yuan, H. Wang, L. Wang, X. Chen, G. Zeng, Y. Wu, Adsorptive removal of methylene blue by rhamnolipid-functionalized graphene oxide from wastewater, Water Res. 67 (2014) 330–344.
[11] D.L. Huang, G.M. Zeng, C.L. Feng, S. Hu, X.Y. Jiang, L. Tang, F.F. Su, Y. Zhang, W. Zeng, H.-L. Liu, Degradation of lead-contaminated lignocellulosic waste by Phanerochaete chrysosporium and the reduction of lead toxicity, Environ. Sci. Technol. 42 (13) (2008) 4946–4951.
[12] G. Zeng, M. Chen, Z. Zeng, Risks of neonicotinoid pesticides, Science 340 (6139) (2013). 1403-1403.
[13] X.D. Du, C.C. Wang, J.G. Liu, X.D. Zhao, J. Zhong, Y.X. Li, J. Li, P. Wang, Extensive and selective adsorption of ZIF-67 towards organic dyes: performance and mechanism, JCIS 506 (Suppl. C) (2017) 437–441.
[14] K. Gupta, O.P. Khatri, Reduced graphene oxide as an effective adsorbent for removal of malachite green dye: plausible adsorption pathways,, JCIS 501 (Suppl. C) (2017) 11–21.
[15] J. Zhao, Q. Huang, M. Liu, Y. Dai, J. Chen, H. Huang, Y. Wen, X. Zhu, X. Zhang, Y. Wei, Synthesis of functionalized MgAl-layered double hydroxides via modified mussel inspired chemistry and their application in organic dye adsorption, JCIS 505 (Suppl. C) (2017) 168–177.
[16] Y. Xue, H. Hou, S. Zhu, Adsorption removal of reactive dyes from aqueous solution by modified basic oxygen furnace slag: isotherm and kinetic study, Chem. Eng. J. 147 (2) (2009) 272–279.
[17] P. Xu, G.M. Zeng, D.L. Huang, C.L. Feng, S. Hu, M.H. Zhao, C. Lai, Z. Wei, C. Huang, G.X. Xie, Use of iron oxide nanomaterials in wastewater treatment: a review, ScTEn 424 (2012) 1–10.

[18] C. Zhang, C. Lai, G. Zeng, D. Huang, C. Yang, Y. Wang, Y. Zhou, M. Cheng, Efficacy of carbonaceous nanocomposites for sorbing ionizable antibiotic sulfamethazine from aqueous solution, Water Res. 95 (2016) 103–112.
[19] J.M. Yang, A facile approach to fabricate an immobilized-phosphate zirconium-based metal-organic framework composite (UiO-66-P) and its activity in the adsorption and separation of organic dyes, JCIS 505 (Suppl. C) (2017) 178–185.
[20] G.Z. Kyzas, E.A. Deliyanni, N.K. Lazaridis, Magnetic modification of microporous carbon for dye adsorption, JCIS 430 (Suppl. C) (2014) 166–173.
[21] M. Cheng, G. Zeng, D. Huang, C. Lai, Z. Wei, N. Li, P. Xu, C. Zhang, Y. Zhu, X. He, Combined biological removal of methylene blue from aqueous solutions using rice straw and Phanerochaete chrysosporium, Appl. Microbiol. Biotechnol. 99 (12) (2015) 5247–5256.
[22] L. Tang, G.M. Zeng, G.L. Shen, Y.P. Li, Y. Zhang, D.-L. Huang, Rapid detection of picloram in agricultural field samples using a disposable immunomembrane-based electrochemical sensor, Environ. Sci. Technol. 42 (4) (2008) 1207–1212.
[23] H. Li, N. An, G. Liu, J. Li, N. Liu, M. Jia, W. Zhang, X. Yuan, Adsorption behaviors of methyl orange dye on nitrogen-doped mesoporous carbon materials, JCIS 466 (Suppl. C) (2016) 343–351.
[24] C. Yang, H. Chen, G. Zeng, G. Yu, S. Luo, Biomass accumulation and control strategies in gas biofiltration, Biotechnol. Adv. 28 (4) (2010) 531–540.
[25] D. Huang, W. Xue, G. Zeng, J. Wan, G. Chen, C. Huang, C. Zhang, M. Cheng, P. Xu, Immobilization of Cd in river sediments by sodium alginate modified nanoscale zero-valent iron: impact on enzyme activities and microbial community diversity, Water Res. 106 (2016) 15–25.
[26] M. Cheng, G. Zeng, D. Huang, C. Lai, P. Xu, C. Zhang, Y. Liu, J. Wan, X. Gong, Y. Zhu, Degradation of atrazine by a novel Fenton-like process and assessment the influence on the treated soil, J. Hazard. Mater. 312 (2016) 184–191.
[27] H. Yi, G. Xu, H. Cheng, J. Wang, Y. Wan, H. Chen, An overview of utilization of steel slag, Proc. Environ. Sci. 16 (2012) 791–801.
[28] I. Blanco, P. Molle, L.E.S. de Miera, G. Ansola, Basic oxygen furnace steel slag aggregates for phosphorus treatment. Evaluation of its potential use as a substrate in constructed wetlands, Water Res. 89 (2016) 355–365.
[29] J. Liang, X.A. Ning, M. Kong, D. Liu, G. Wang, H. Cai, J. Sun, Y. Zhang, X. Lu, Y. Yuan, Elimination and ecotoxicity evaluation of phthalic acid esters from textile-dyeing wastewater, Environ. Pollut. 231 (Part 1) (2017) 115–122.
[30] J.L. Parrott, A.J. Bartlett, V.K. Balakrishnan, Chronic toxicity of azo and anthracenedione dyes to embryo-larval fathead minnow, Environ. Pollut. 210 (Suppl. C) (2016) 40–47.
[31] S. Largergren, Zur theorie der sogenannten adsorption geloster stoffe. Kungliga Svenska Vetenskapsakademiens, Handlingar 24 (4) (1898) 1–39.
[32] Y.S. Ho, G. McKay, Kinetic models for the sorption of dye from aqueous solution by wood, Process Saf. Environ. Prot. 76 (2) (1998) 183–191.
[33] I. Lanowix, The adsorption of gases on plane surface of glass, mica and platinum, J. Am. Chem. Soc. 30 (1918) 1361.
[34] H. Freundlich, Uber die adsorption in losungen, Z. Phys. Chem. 57 (1906) 385.
[35] J. Wang, S. Xing, Y. Huang, P. Fan, J. Fu, G. Yang, L. Yang, P. Lv, Highly stable gasified straw slag as a novel solid base catalyst for the effective synthesis of biodiesel: Characteristics and performance, ApEn 190 (2017) 703–712.
[36] J. Lalley, C. Han, X. Li, D.D. Dionysiou, M.N. Nadagouda, Phosphate adsorption using modified iron oxide-based sorbents in lake water: kinetics, equilibrium, and column tests, Chem. Eng. J. 284 (2016) 1386–1396.
[37] H. Gao, Z. Song, W. Zhang, X. Yang, X. Wang, D. Wang, Synthesis of highly effective absorbents with waste quenching blast furnace slag to remove Methyl Orange from aqueous solution, JEnvS (2016).
[38] T. Fan, Y. Liu, B. Feng, G. Zeng, C. Yang, M. Zhou, H. Zhou, Z. Tan, X. Wang, Biosorption of cadmium (II), zinc (II) and lead (II) by Penicillium simplicissimum: isotherms, kinetics and thermodynamics, J. Hazard. Mater. 160 (2) (2008) 655–661.
[39] L. Fernandez, C. Alonso, A. Hidalgo, C. Andrade, The role of magnesium during the hydration of C3S and CSH formation. Scanning electron microscopy and mid-infrared studies, Adv. Cement Res. 17 (1) (2005) 9–21.
[40] J.A. Gadsden, Infrared Spectra of Minerals and Related Inorganic Compounds, Butterworths, 1975.
[41] Y. Cheng, H. He, C. Yang, G. Zeng, X. Li, H. Chen, G. Yu, Challenges and solutions for biofiltration of hydrophobic volatile organic compounds, Biotechnol. Adv. 34 (6) (2016) 1091–1102.
[42] X.-J. Hu, J.-S. Wang, Y.-G. Liu, X. Li, G.-M. Zeng, Z.-L. Bao, X.-X. Zeng, A.-W. Chen, F. Long, Adsorption of chromium (VI) by ethylenediamine-modified cross-linked magnetic chitosan resin: isotherms, kinetics and thermodynamics, J. Hazard. Mater. 185 (1) (2011) 306–314.
[43] Y. Feng, J.-L. Gong, G.-M. Zeng, Q.-Y. Niu, H.-Y. Zhang, C.-G. Niu, J.-H. Deng, M. Yan, Adsorption of Cd (II) and Zn (II) from aqueous solutions using magnetic hydroxyapatite nanoparticles as adsorbents, Chem. Eng. J. 162 (2) (2010) 487–494.
[44] J. Duan, B. Su, Removal characteristics of Cd (II) from acidic aqueous solution by modified steel-making slag, Chem. Eng. J. 246 (2014) 160–167.
[45] M. Cheng, G. Zeng, D. Huang, C. Yang, C. Lai, C. Zhang, Y. Liu, Advantages and challenges of Tween 80 surfactant-enhanced technologies for the remediation of soils contaminated with hydrophobic organic compounds, Chem. Eng. J. 314 (2017) 98–113.
[46] Y. Yao, F. Xu, M. Chen, Z. Xu, Z. Zhu, Adsorption behavior of methylene blue on carbon nanotubes, Bioresour. Technol. 101 (9) (2010) 3040–3046.
[47] J. Yener, T. Kopac, G. Dogu, T. Dogu, Dynamic analysis of sorption of methylene blue dye on granular and powdered activated carbon, Chem. Eng. J. 144 (3) (2008) 400–406.
[48] H.A. Shawky, A.H.M. El-Aassar, D.E. Abo-Zeid, Chitosan/carbon nanotube composite beads: preparation, characterization, and cost evaluation for mercury removal from wastewater of some industrial cities in Egypt, J. Appl. Polym. Sci. 125 (S1) (2012).
[49] W. Liu, J. Zhang, C. Zhang, Y. Wang, Y. Li, Adsorptive removal of Cr (VI) by Fe-modified activated carbon prepared from Trapa natans husk, Chem. Eng. J. 162 (2) (2010) 677–684.